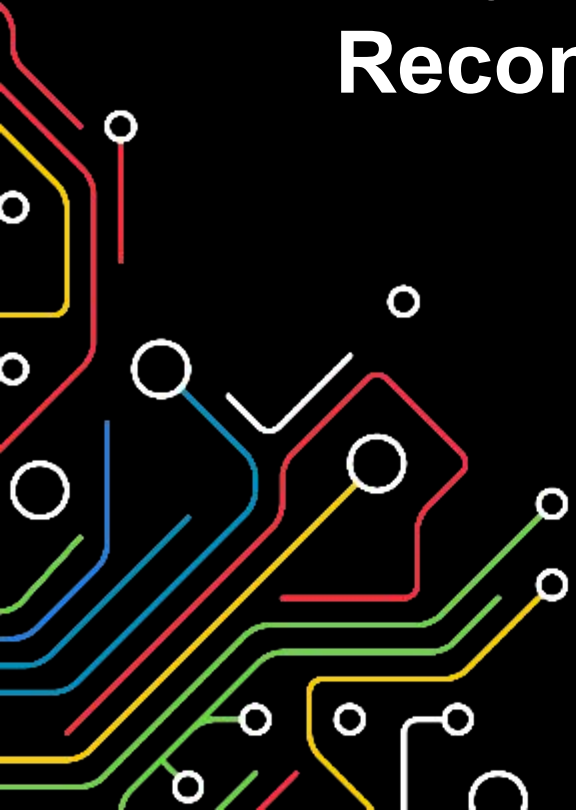


# Human Activity Recognition with a 6.5 GHz Reconfigurable Intelligent Surface for Wi-Fi 6E

NOVEMBER 2024

from knowledge  
generation to  
science-based  
innovation



- **Introduction**
- **Human Activity Recognition**
- **Reconfigurable Intelligent Surfaces**
- **HAR via RIS for WiFi-6E**
  - Modeling the Setup
  - Channel Model
  - Unit Cell & 64-element RIS Implementation
- **Experiments**
  - RIS Validation and Beam Steering
  - Human Hand Gesture Recognition

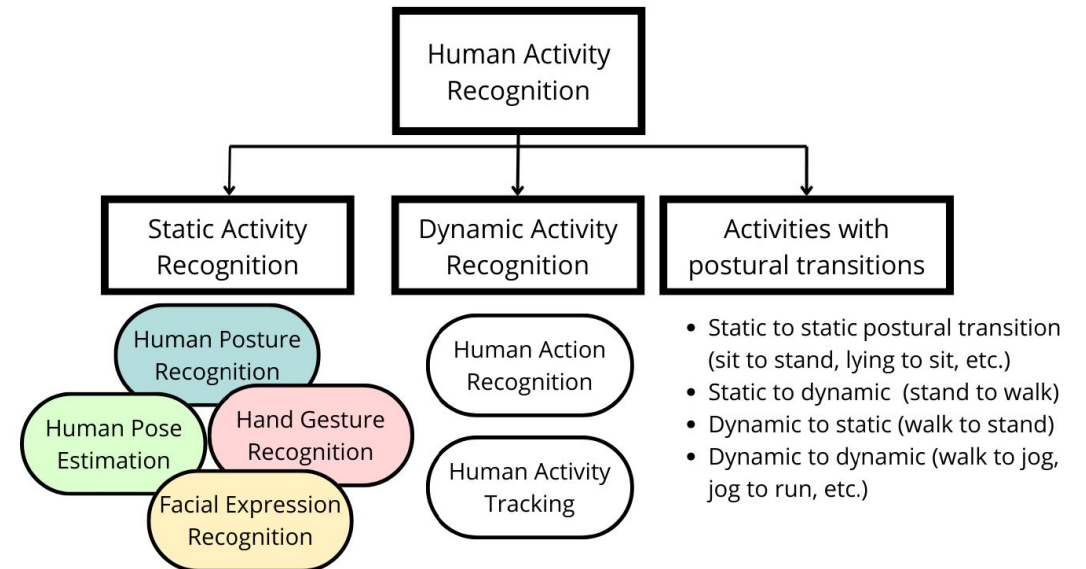
# Human Activity Recognition

- **What is HAR?**

- Identify or classify activities (sitting, walking, falling)
- Typically done with vision or sensor data

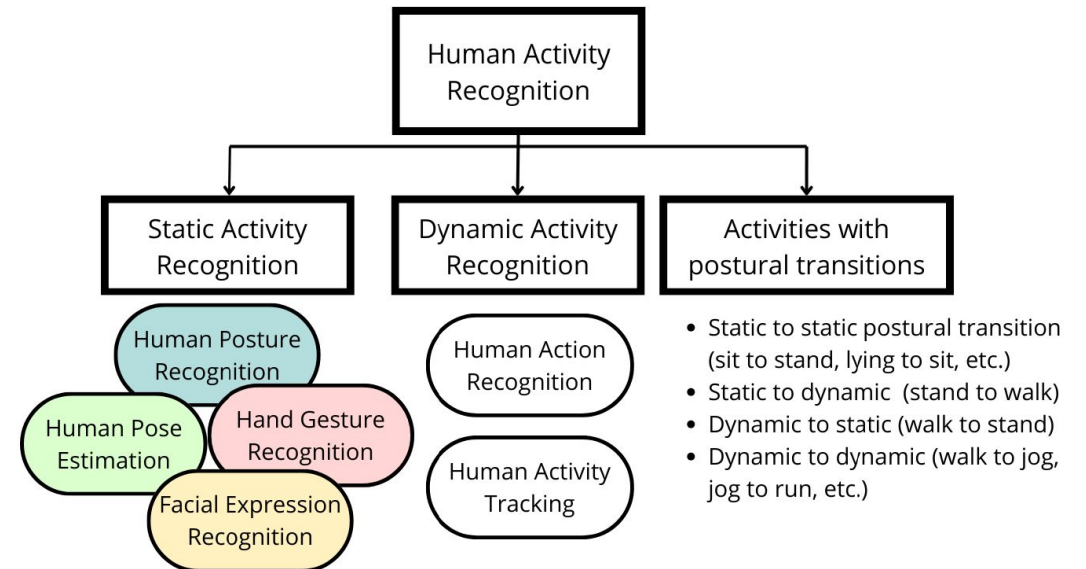
- **Applications**

- Healthcare (Patient monitoring)
- Smart Environments (Home assistance)
- Security (Surveillance systems)
- HCI (Intuitive interfaces)
- XR/AR/VR



# Human Activity Recognition

- **HAR Challenges?**
  - Data Collection and Fusion
  - Feature extraction
  - Sensor Cost
- **RF-Based HAR**
  - Novel approach
  - Exploits stray RF signals in medium
  - Cheaper and privacy capable
  - **But RF medium is generally uncontrollable**



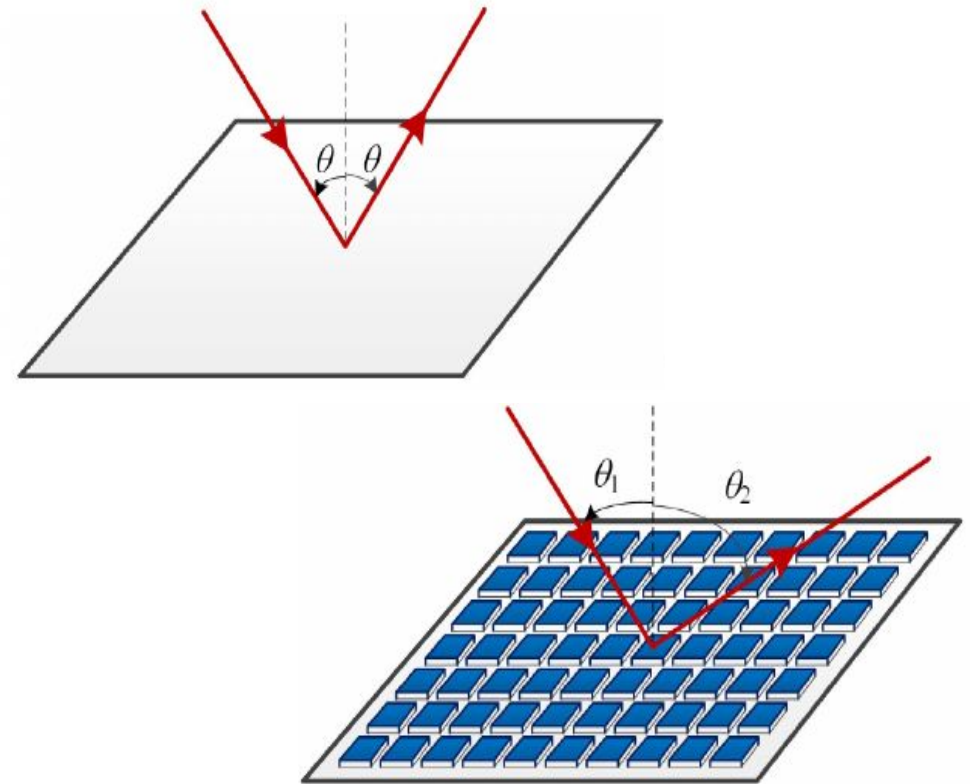
# Reconfigurable Intelligent Surfaces

- **RIS**

- RISs are 2D matrices of passive antenna elements (unit cells) that **reflect** RF signals.
- Each unit cell adjusts the **reflection coefficient** to control signal **phase** and **direction**.

- Key Points

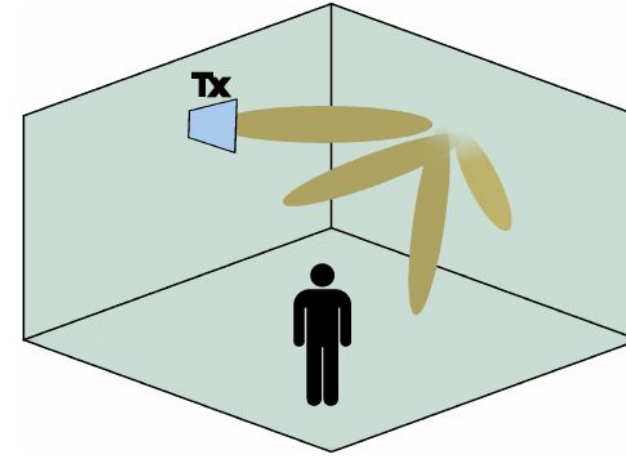
- No active RF chains – low power and cost.
- Capable of **non-specular** reflections
- Promising as solution for challenges in 6G and high-frequency band



# Reconfigurable Intelligent Surfaces

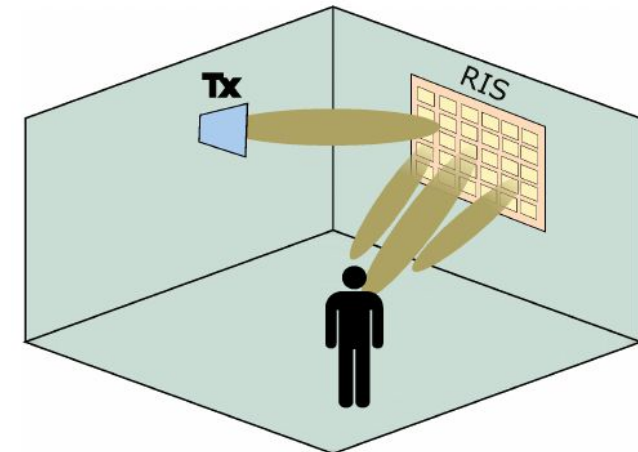
- **Controllable medium**

- Non-specular reflections
- NLoS channels
  - Extended coverage
  - Indoor environments
- Localization
- Sensing



- **RF-Based HAR with RIS**

- Medium is controllable through manipulation of reflected signals
- Associates medium response to control and status of medium → sensing
- High spatial resolution



# Contributions

- Design of a PIN diode based unit cell for 6.5 GHz
- Design of a RIS with 64 elements
- Modeled the environment and channel for an Hand Gesture Recognition
- Implemented RIS configuration for sensing
- Dataset for RF-based classification human gestures
- Classification of gestures for two different CNNs

# RIS-Based Hand Gesture Recognition (HGR)

Why 6.5GHz RIS?

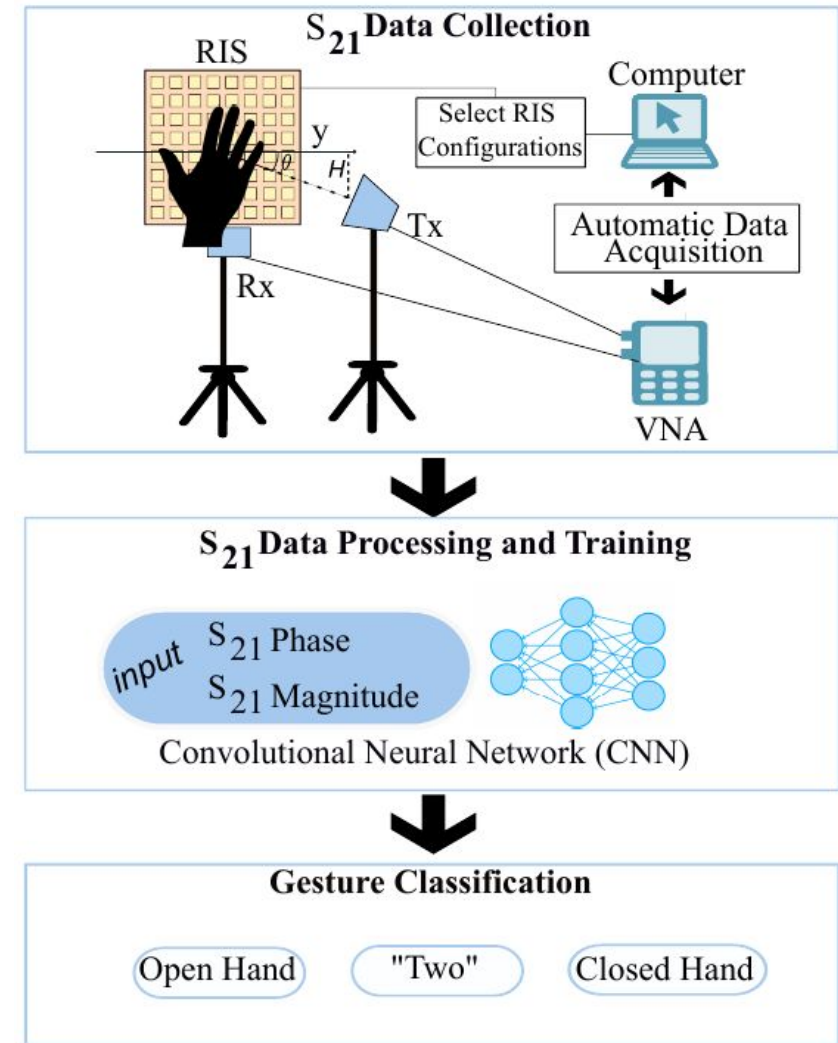
- Leverage ubiquity of WiFi and higher spatial resolution of higher frequency

Why Hand Gesture Recognition?

- Suitable for our RIS size of  $18\text{cm}^2$

## Overall Approach

1. Gather  $S_{21}$  parameters in chamber
2. Represent data as image-like tensors
3. Train CNN and classify gestures

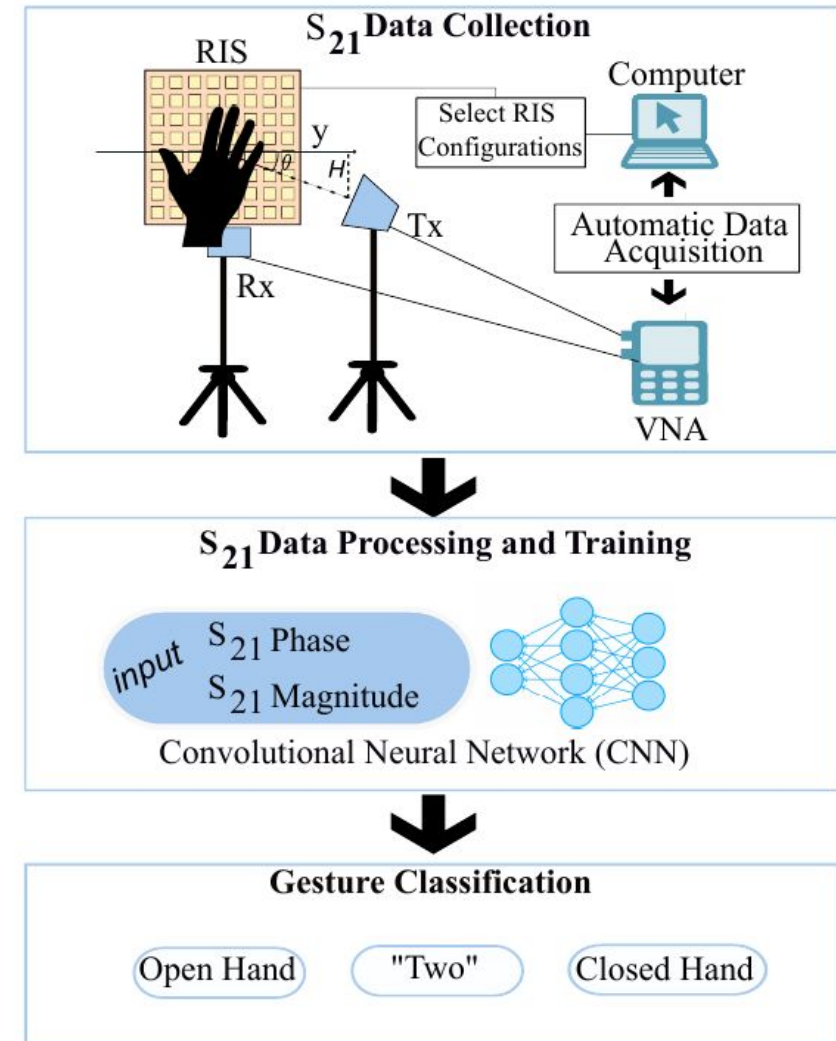




# RIS-Based Hand Gesture Recognition (HGR)

Gather  $S_{21}$  parameters in chamber

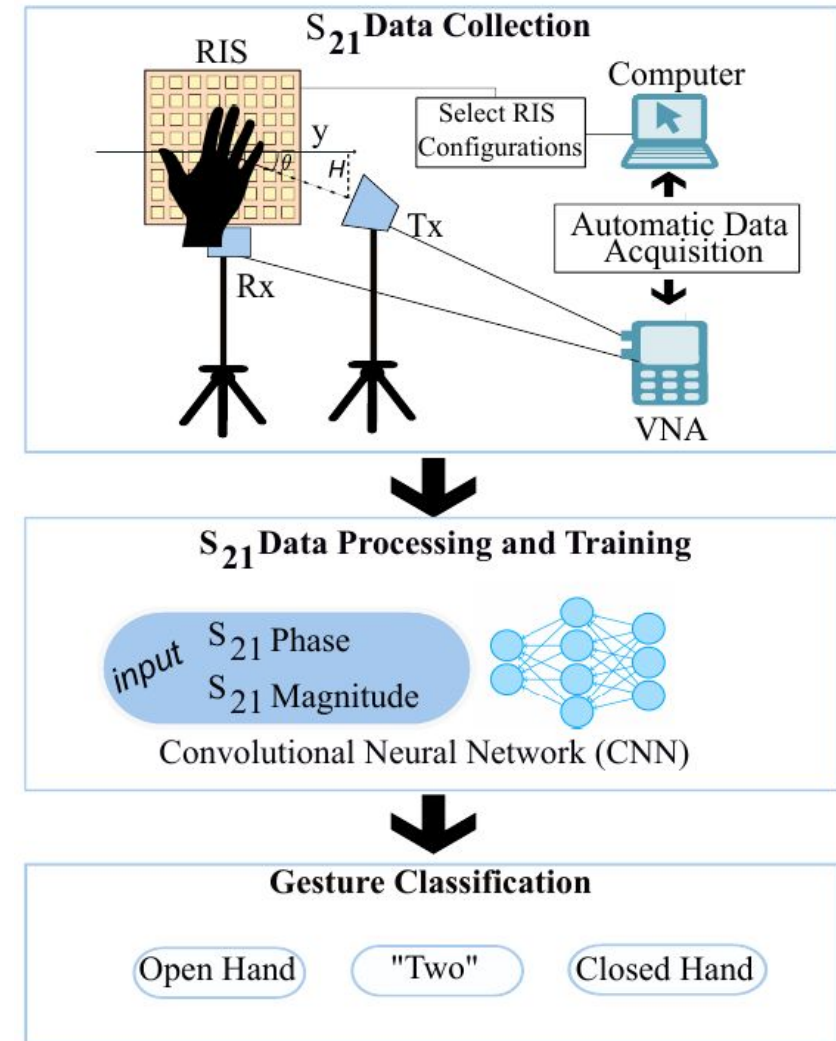
- Anechoic chamber
- Signal path (sequence):
  - Transmitter (Tx).
  - RIS
  - Space of Interest (Sol)
  - Receiver (Rx)



# RIS-Based Hand Gesture Recognition (HGR)

Gather  $S_{21}$  parameters in chamber

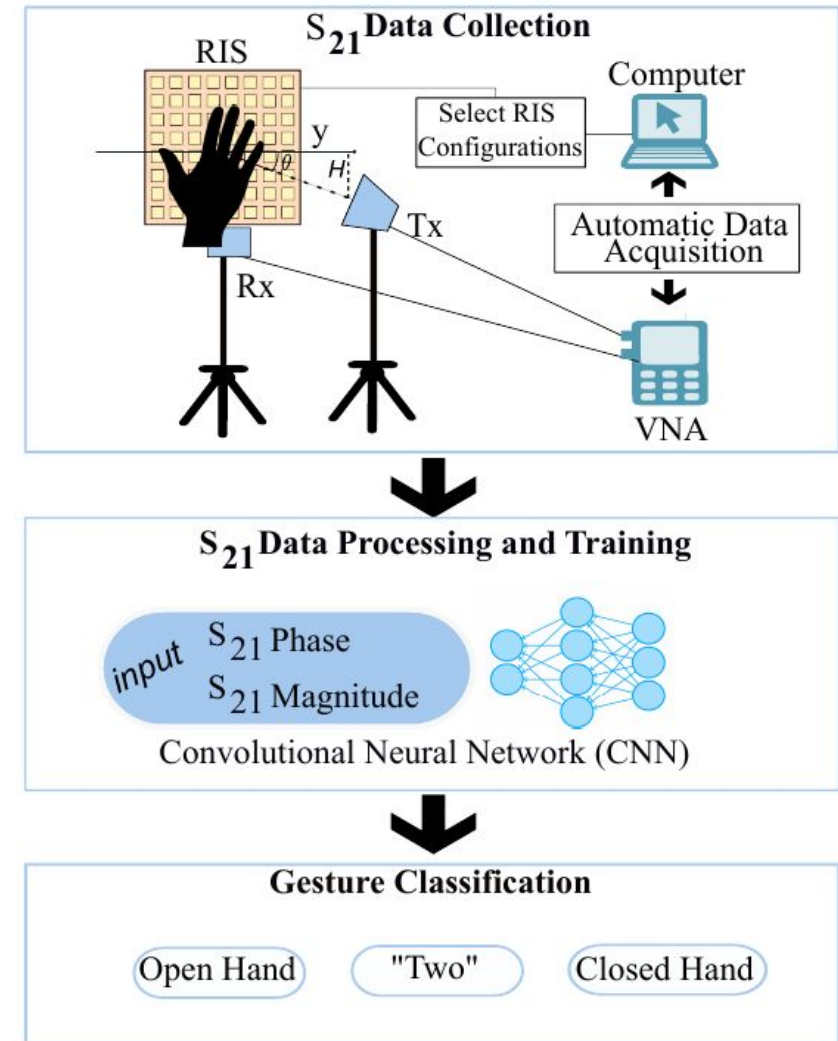
- Sol (Space-of-Interest) → Hand gestures
- Hand gestures → Different  $S_{21}$  data
- $S_{21}$  parameters measured with VNA
- For two RIS configuration methods:
  - Random sequences
  - Optimized sequences



# RIS-Based Hand Gesture Recognition (HGR)

## Image representation and classification

- From S21 data:
  - $xx$  axis  $\rightarrow$  RIS configuration
  - $yy$  axis  $\rightarrow$  Frequency range
  - Color value  $\rightarrow$ 
    - 1) Phase or 2) Mag. response
    - $\rightarrow$  i.e., two channels
- Feed image channels into CNN



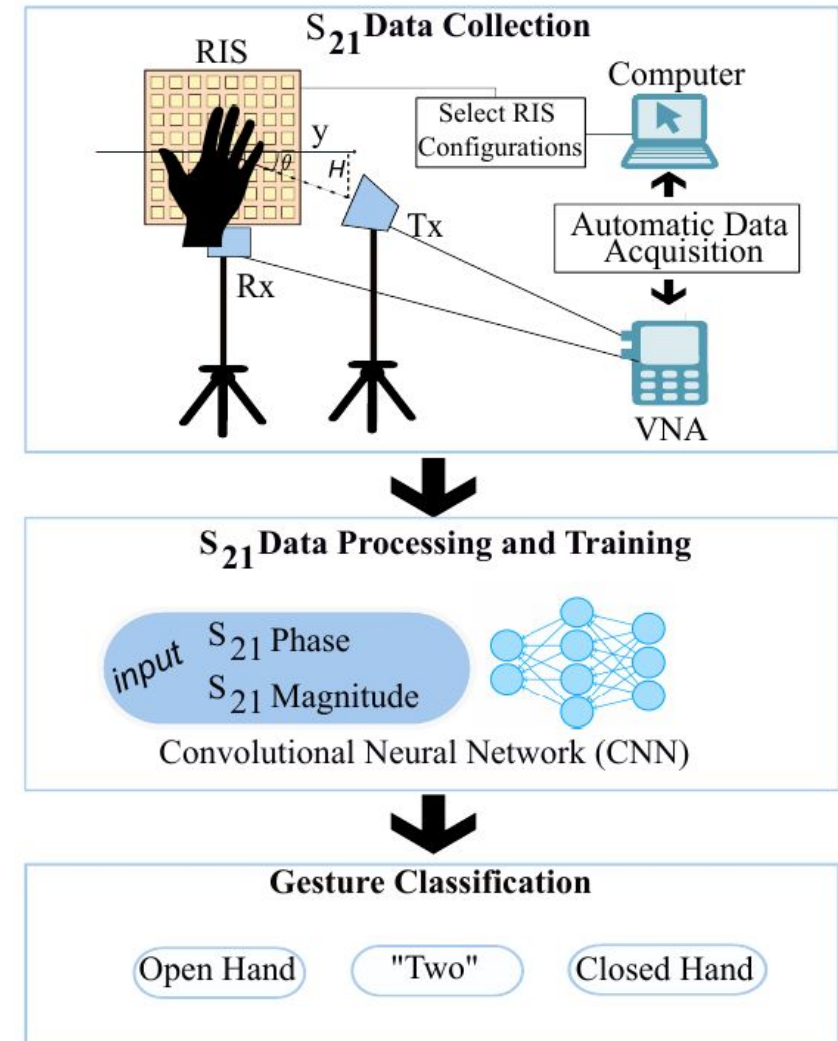
# RIS-Based Hand Gesture Recognition (HGR)

## Setup

1. Physical setup for HGR
2. Channel model and RIS configuration

## Experiments

3. Unit cell characterization
4. RIS steering validation
5. Feasibility study of HGR with RIS
6. RIS-based HGR Classification



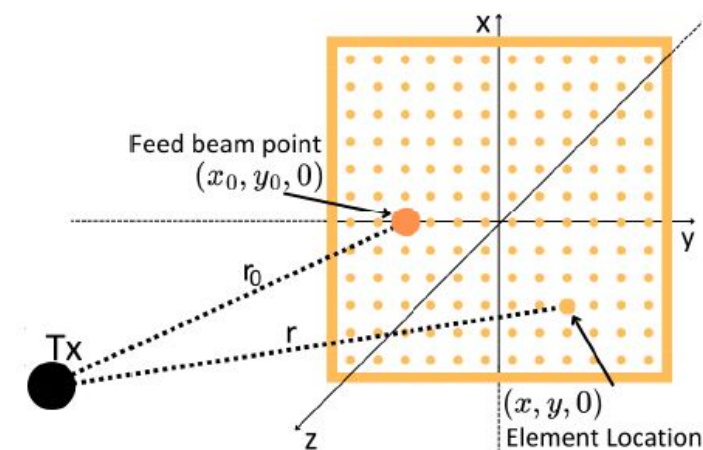
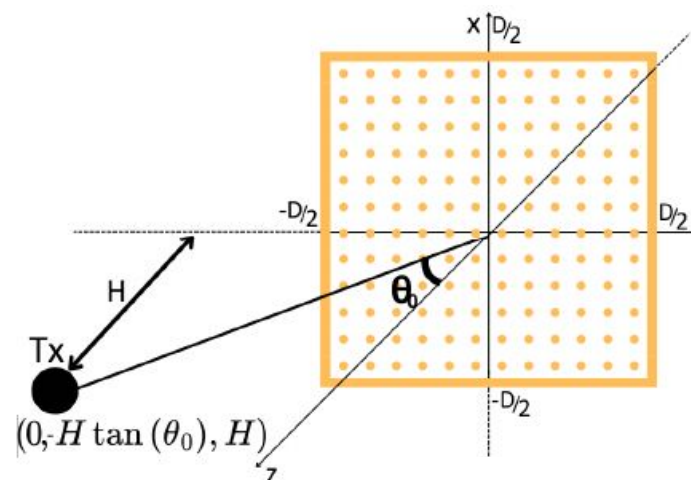
# Setup: Physical Setup for HGR

## Model

- RIS is coordinate origin
- TX at:
  - Offset angle  $\theta$
  - Distance  $H$
- Rx and Tx are horn antennas

## Issue

- Maximize illumination of RIS by the TX  $\rightarrow$  find  $\mathbf{H}$  and  $\boldsymbol{\theta}$
- Reduce occlusion of RIS by TX



# Setup: Physical Setup for HGR

## Maximize illumination

- Spillover Efficiency ( $\eta_s$ )
- Illumination Efficiency ( $\eta_i$ )
- Maximize  $\eta_a = \eta_s \times \eta_i$

## Swept parameters

- $\theta_0$ :  $0^\circ$  to  $50^\circ$
- $H$ : 20 cm to 180 cm
- $y_0$ :  $\pm 15$  cm

## Results

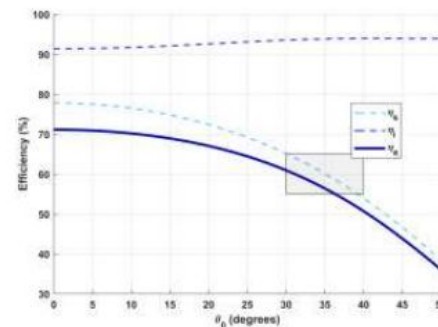
- $\theta_0 = 35^\circ$ ,  $H = 33$  cm.
- 35% total efficiency ( $\eta_a$ ) due to chamber constraints.

$$\eta_s = \frac{\iint_A P(r) dA}{\iint_{\text{sphere}} P(r) dA} \quad (1)$$

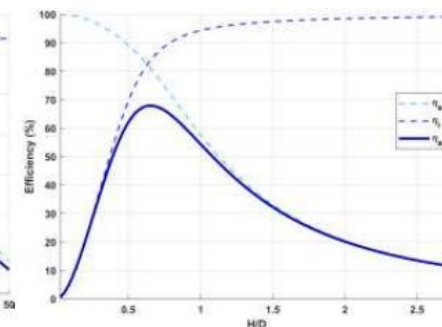
$$P(r)dA = \frac{H}{r^3} \left( \frac{r_0^2 + r^2 - s^2}{2r_0r} \right)^{2q} dx dy \quad (2)$$

$$\eta_i = \frac{1}{A} \frac{|\iint_A I(x, y) dA|^2}{\iint_A |I(x, y)|^2 dA} \quad (3)$$

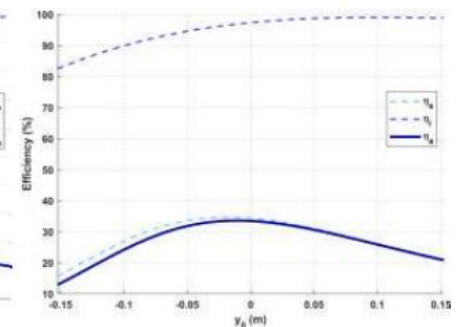
$$I(x, y) = \frac{H^{q_e}}{r^{1+q_e}} \left( \frac{r_0^2 + r^2 - s^2}{2r_0r} \right)^q \quad (4)$$



(a) function of  $\theta_0$



(b) function of  $H/D$



(c) function of  $y_0$



# Setup: Physical Setup for HGR

**Tx Position** → Determined

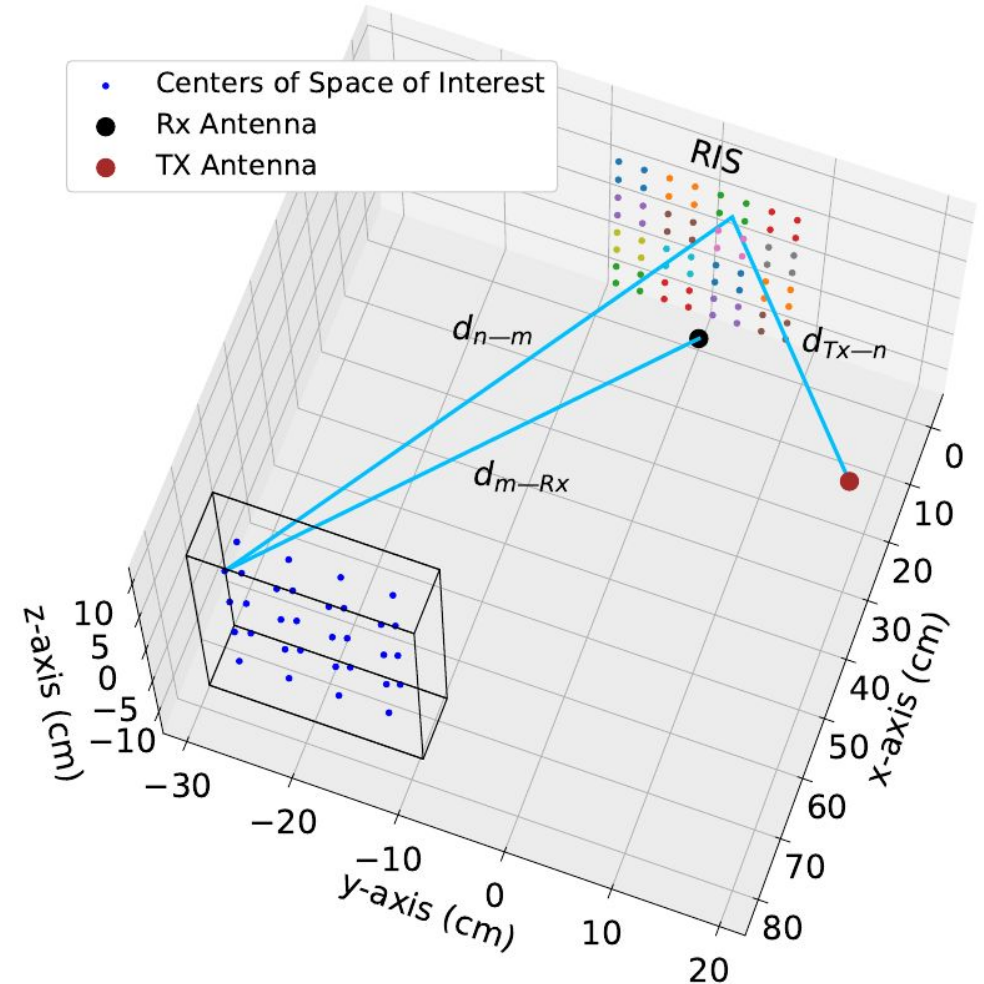
**Sol?**

- 15° offset to minimize Tx interference
- Divided into  $M=32$  equal cuboids

**Rx Positioning?**

- Rx positioned directly below RIS

Effective configuration despite physical limitations of chamber.



# Setup: Channel Model

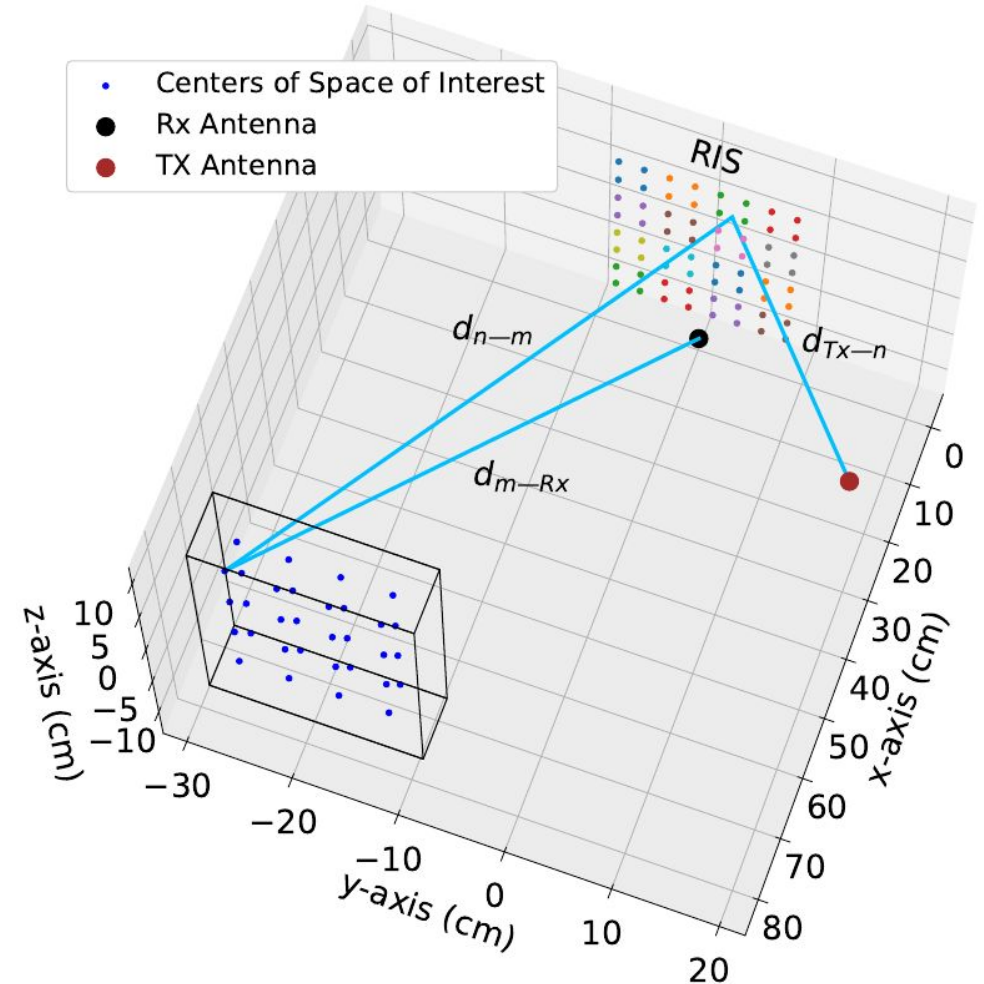
## Components of the Model

- Tx Sends signals to the RIS
- **RIS**
  - 64 elements divided into 16 groups ( $L = 16$ )
  - Groups of 4 elements controlled jointly
- **Space-of-Interest (Sol):**
  - Divided into 32 cuboids ( $M = 32$ ).
  - Gesture  $\rightarrow$  Reflection coefficient  $\eta_m$  varies
- **Receiver (Rx)**
  - Captures reflected signals from Sol.

What is the total received Rx signal  $y_{rx}$ ?

What is the channel gain  $h$ ?

How does RIS configuration change  $y_{rx}$ ?





# Setup: Channel Model

## Total signal $y_{rx}$

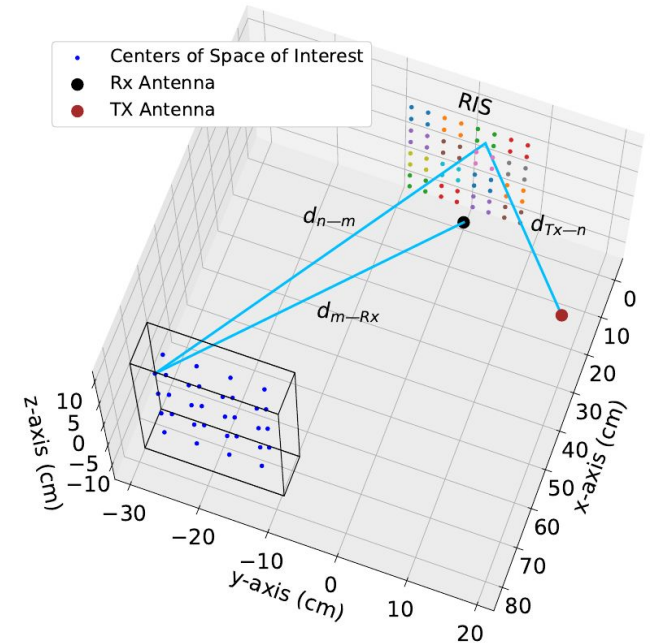
- Reflections from each unit cell to each cuboid
- Reflections from each cuboid to Rx

$$y_{rx} = \sum_{m \in [1, M]} \sum_{l \in [1, L]} \sum_{n \in \mathcal{N}_l} h_{n,m}(s_l, \eta_m) \cdot P_t \cdot x$$

- $P_t$  is Tx power
- $x$  is baseband signal at  $f_c$
- $h$  is channel gain
  - $\eta_m$  depends on Sol state
  - $S_l$  is configuration of group of cells

$\eta_m$ :  
 $r_n, m$ :  
 $g_T, g_R$ :  
 $d_{nTx}$ :  
 $d_{nm}$ :  
 $d_{mRx}$ :

reflection coefficient of each cuboid  
 RIS's reflection coefficients  
 transmitter/receiver gains  
 Distance from Tx to RIS element  $n$ .  
 Distance from RIS element  $n$  to Sol cuboid  $m$ .  
 Distance from Sol cuboid  $m$  to Rx.



# Setup: Channel Model

## Modeling channel gain ( $h$ )

- SoA reflection formula
- Derive distances from physical model layout

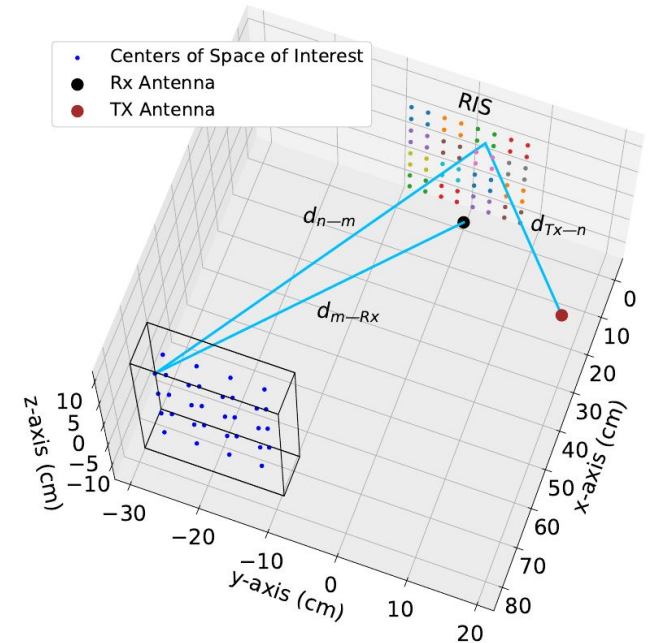
$$\phi_{n,m} = e^{-j2\pi(d_{nTx} + d_{nm} + d_{mRx})/\lambda}$$

$$h_{n,m}(s_l, \eta_m) = \frac{\lambda \cdot r_{n,m}(s_l) \cdot \eta_m \cdot \sqrt{g_T \cdot g_R}}{4\pi \cdot d_{nTx} \cdot d_{nm} \cdot d_{mRx}} \cdot \phi_{n,m}$$

- $r_{n,m}$  is the impedance response of the unit cell at  $\mathbf{n}, \mathbf{m}$
- Impedance depends on configuration  $\mathbf{S}_l$

$\eta_m$ :  
 $r_{n,m}$ :  
 $g_T, g_R$ :  
 $d_{nTx}$ :  
 $d_{nm}$ :  
 $d_{mRx}$ :

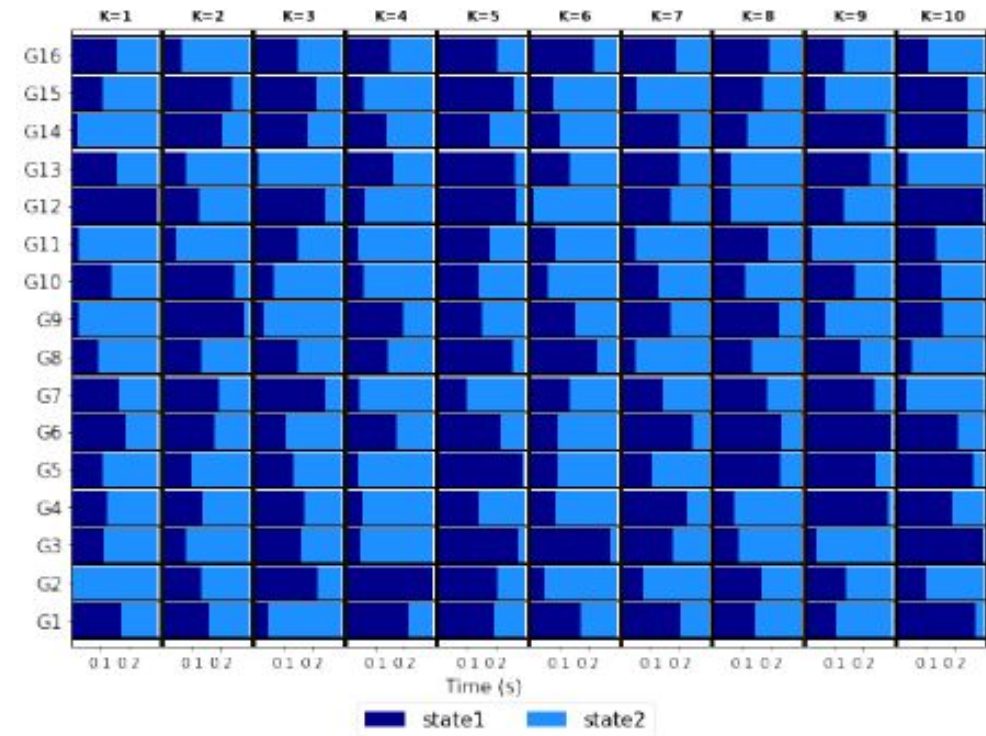
reflection coefficient of each cuboid  
 RIS's reflection coefficients  
 transmitter/receiver gains  
 Distance from Tx to RIS element  $n$ .  
 Distance from RIS element  $n$  to Sol cuboid  $m$ .  
 Distance from Sol cuboid  $m$  to Rx.



# Setup: RIS Configuration Sequence

## RIS Reconfiguration

- RIS configuration → known
- Sol state → unknown
- Sequences of RIS states produce different S21 responses
  - i.e., we are “observing” the unknown state from several “perspectives”
- We consider 10 “frames” where each of the 16 cells changes state



Time vs. state for 16 cells

# Setup: RIS Configuration Sequence

## Modeling Config. Sequence

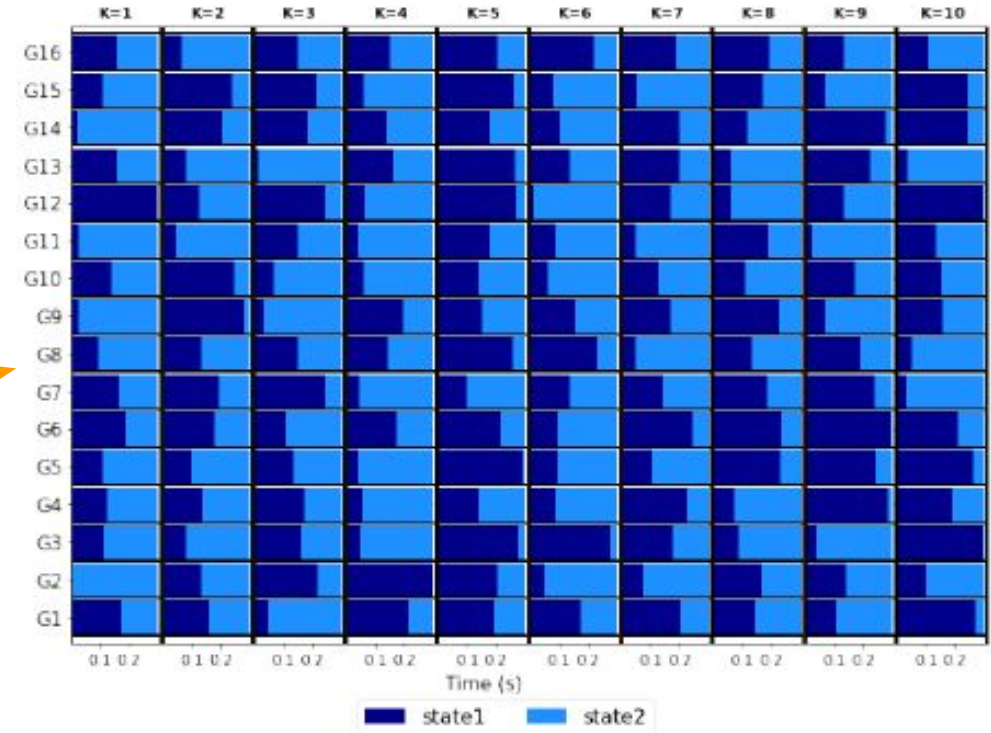
- RIS elements transition between states ( $s_1, s_{N_a}$ ) per time frame ( $\delta$ ).
- 1-bit RIS (2 states)**

$$T = (t_1 \quad t_2 \quad \dots \quad t_K)^T$$

$$A = [\alpha_1 \quad \alpha_2 \quad \dots \quad \alpha_M]$$

channel gains  
for cell states

$$y_{rx} = P_t \cdot x \cdot T \cdot A \cdot \eta, \quad \text{with } \Gamma = T \cdot A$$



Time vs. state for 16 cells

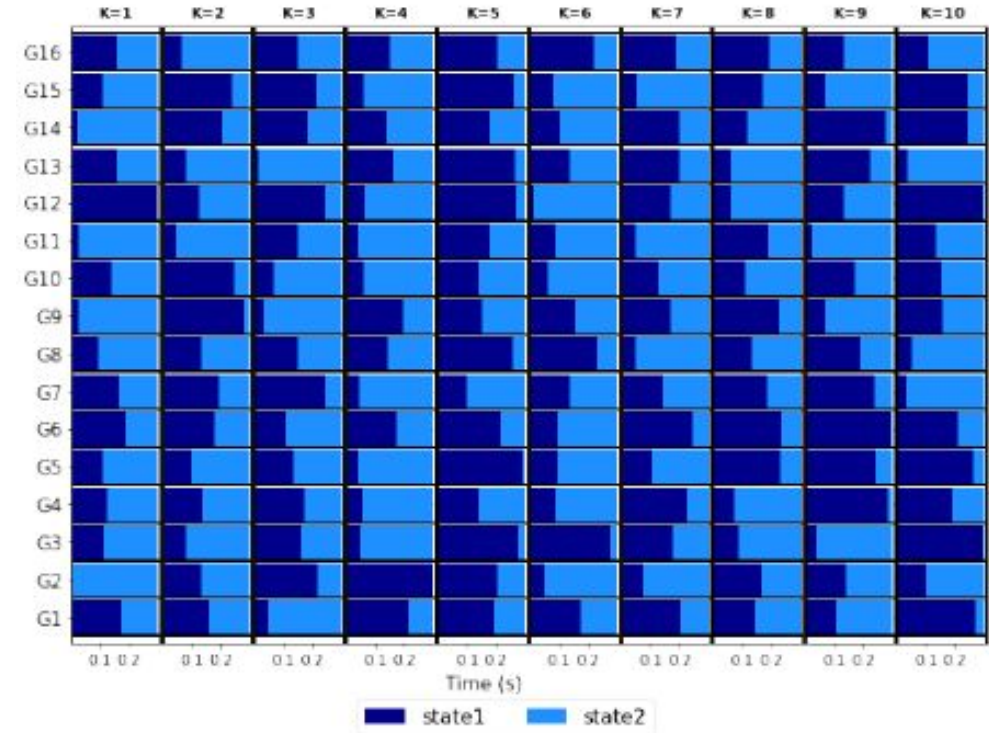
$\Gamma = T \cdot A$ : **Combines RIS configurations and channel gain matrix.**

# Setup: RIS Configuration Sequence

## Determining the Sequence

- Can be random
- However
  - May lead to redundant or insufficient data
  - Ideally, signal paths should carry uncorrelated information
  - Use optimized configurations

→ Optimize for minimum mutual coherence using SoA algorithm



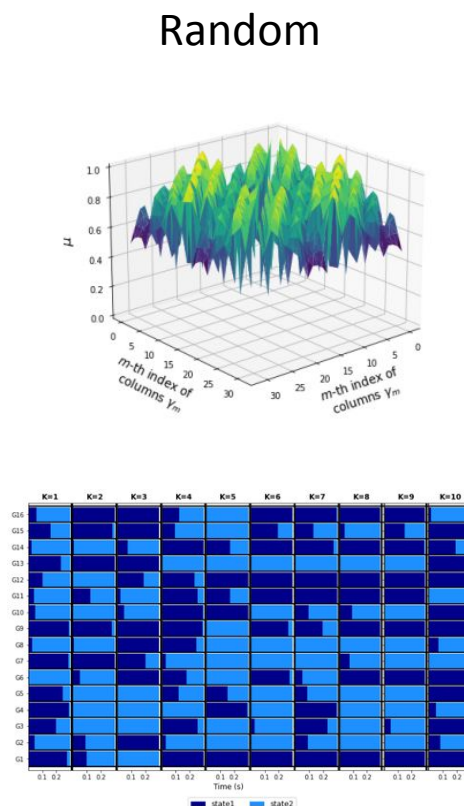
Time vs. state for 16 cells



# Setup: RIS Configuration Sequence

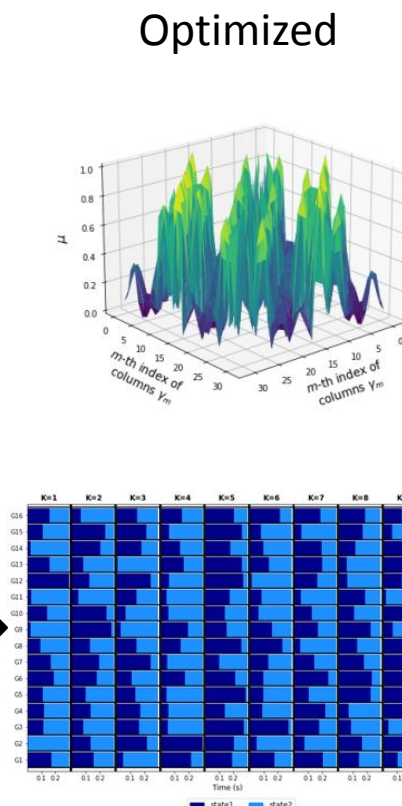
## Optimizing the Sequence

- FCAO Algorithm
- Minimizes mutual coherence
- Sequence gathers more Sol information



$$\begin{aligned}
 (P1) \min_T & \mu(T), \\
 \text{with } & \gamma_m = t_k \alpha_m, \quad \forall m \in [1, M], \\
 & \mathbf{1}^T \tilde{t}_{k,l} = \delta, \quad \forall k \in [1, K], l \in [1, L], \\
 & \tilde{t}_{k,l,i} \geq 0, \quad \forall k \in [1, K], l \in [1, L], i \in [1, N_d].
 \end{aligned}$$

$$\begin{aligned}
 (P2) \min_{\tilde{t}_{k,l}, u} & \|\mathbf{u}\|_1, \\
 \text{s.t. } & u_{m,m'} = \frac{\gamma_m^T \gamma_{m'}}{\|\gamma_m\|_2 \cdot \|\gamma_{m'}\|_2}, \\
 & m, m' \in [1, M], m \neq m', \\
 & \mathbf{1}^T \tilde{t}_{k,l} = \delta, \quad \forall l \in [1, L], \\
 & \tilde{t}_{k,l} \geq 0, \quad \forall l \in [1, L],
 \end{aligned}$$



Mutual Coherence

Frame Configuration matrix T

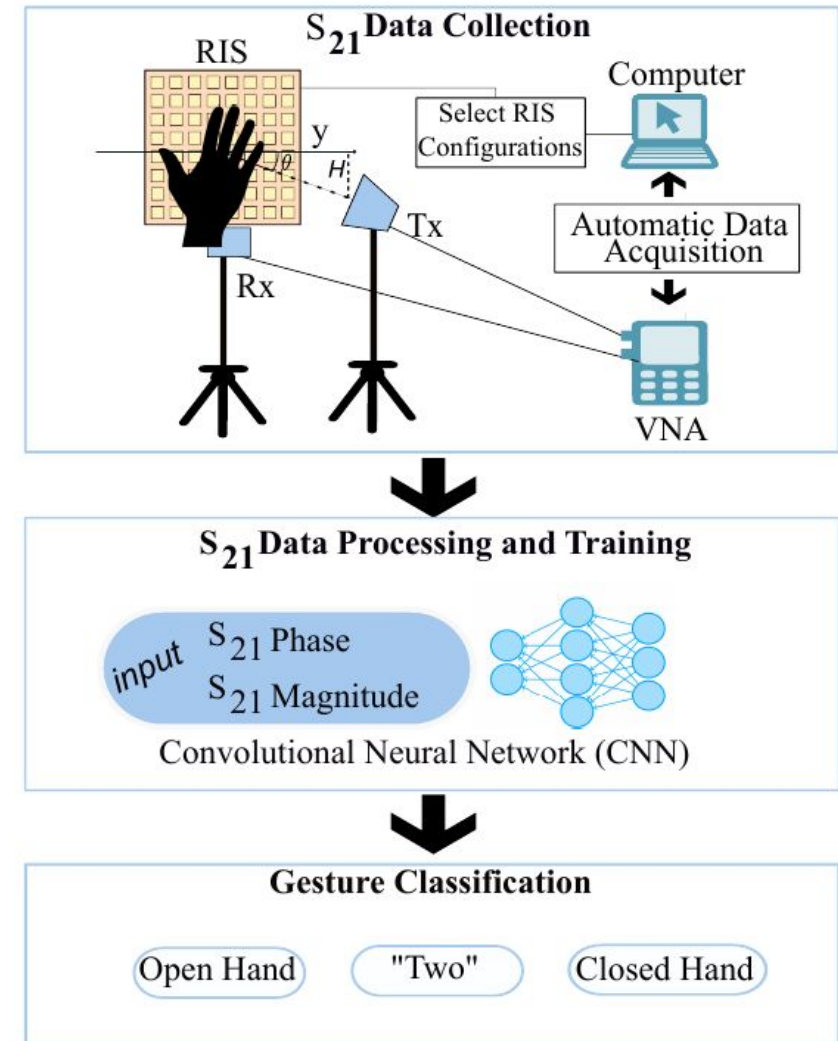
# RIS-Based Hand Gesture Recognition (HGR)

## Setup

1. ~~Physical setup for HGR~~
2. ~~Channel model and RIS configuration~~

## Experiments

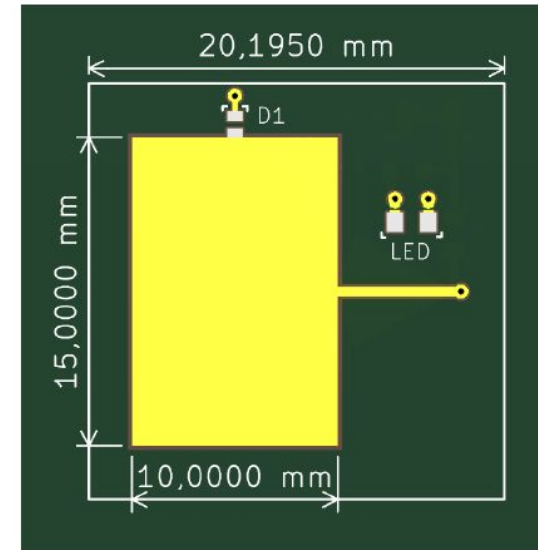
3. **Unit cell characterization**
4. RIS steering validation
5. Feasibility study of HGR with RIS
6. RIS-based HGR Classification



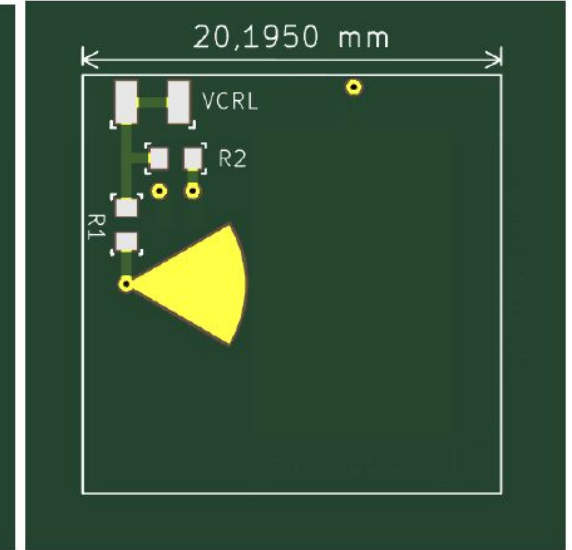
# PIN Based Unit Cell Design

## Unit Cell for 6.5GHz

- Simple patch antenna
  - $f_c = 6.5$  GHz, central to the WiFi-6E band
  - 10mm x 15 mm
  - Vertical polarization
  - 4mm F4B + 0.5 FR4 substrate
- Impedance Control
  - PIN diode (SMP1331-079LF)
  - 0.8V forward bias
  - For VCTRL = 3.3V  $\rightarrow$  15mA draw



(a) top layer



(b) bottom layer

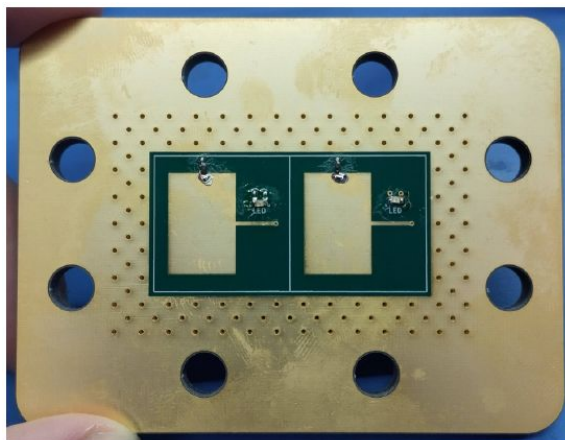


# PIN Based Unit Cell Design

**Objective:** Compare fabricated unit cell performance to CST simulation.

## Experimental Setup

PCB with two unit cells in WR159 waveguide. Measure S11 in VNA.

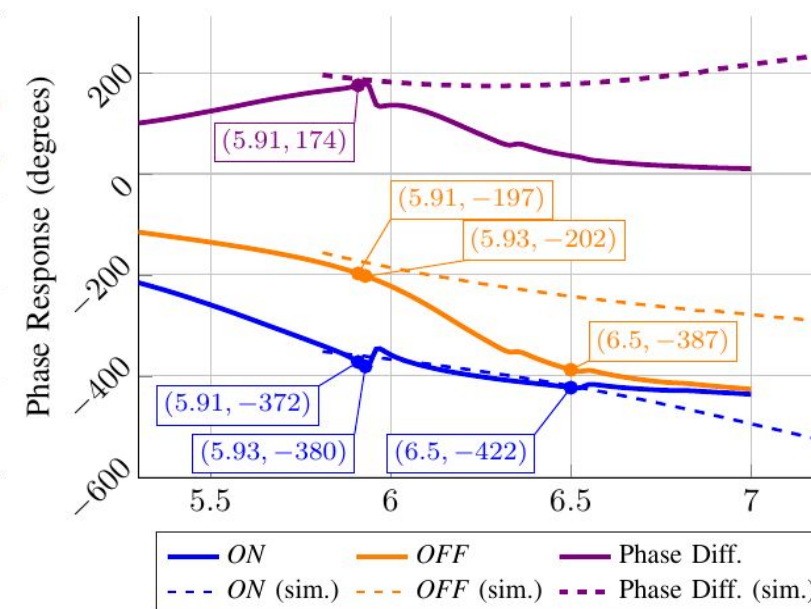
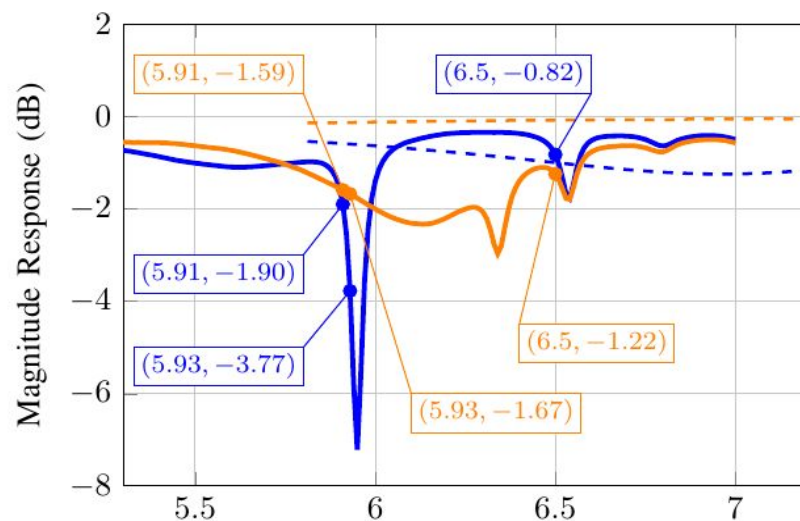


## Experimental Results

- Simulations predicted 180° phase shift at 6.5 GHz; measured 35°.
- Best trade-off at 5.91 GHz with 174° phase shift and balanced magnitude response.

## Conclusion

- Phase difference 35° at 6.5GHz
- Phase difference 178° at 5.93 GHz but magnitude disparity
- **Use 5.91 GHz** for balanced magnitude response and 174° phase difference.



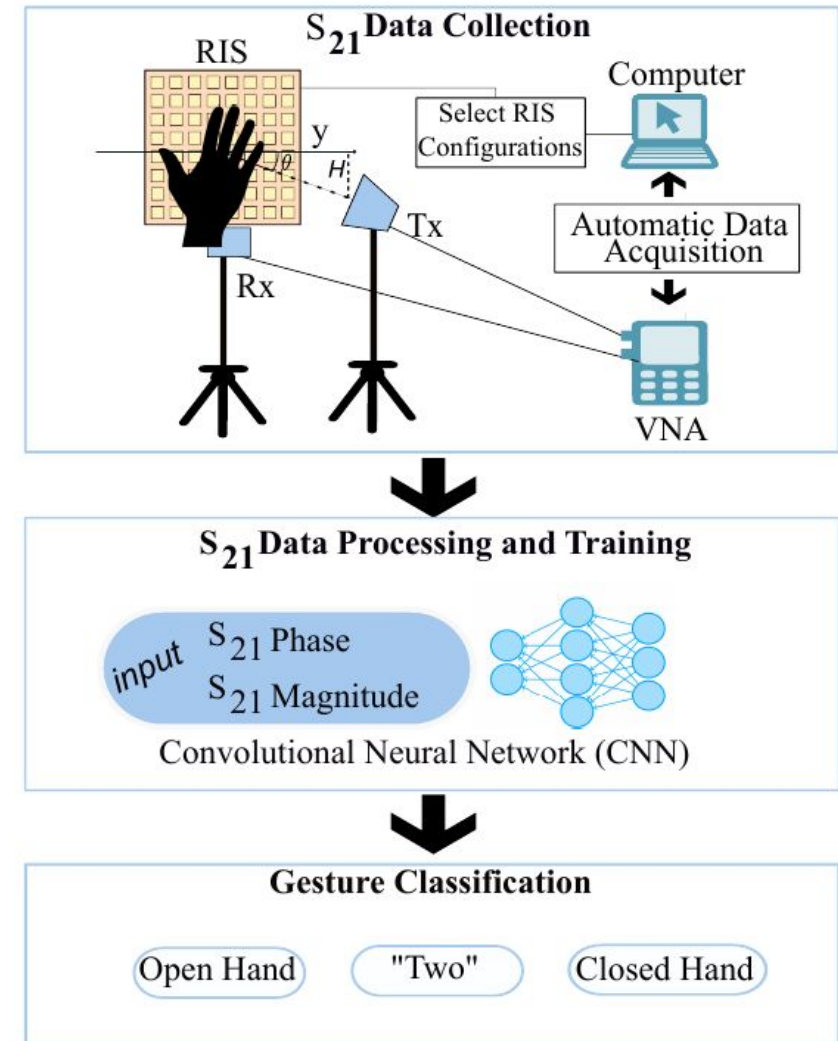
# RIS-Based Hand Gesture Recognition (HGR)

## Setup

- ~~1. Physical setup for HGR~~
- ~~2. Channel model and RIS configuration~~

## Experiments

- ~~3. Unit cell characterization~~
- 4. RIS steering validation**
5. Feasibility study of HGR with RIS
6. RIS-based HGR Classification



# 8×8 RIS Tile Design and Beamforming

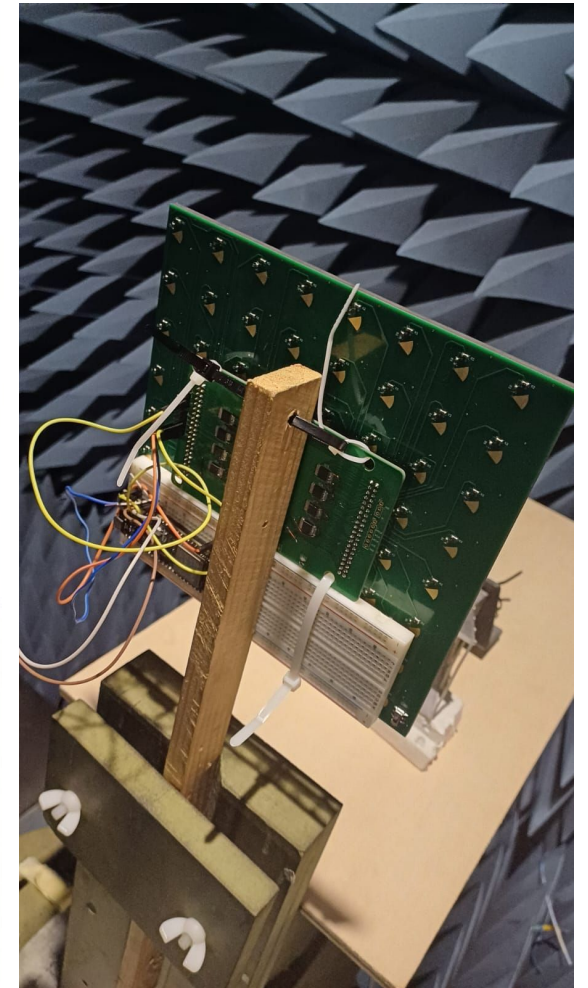
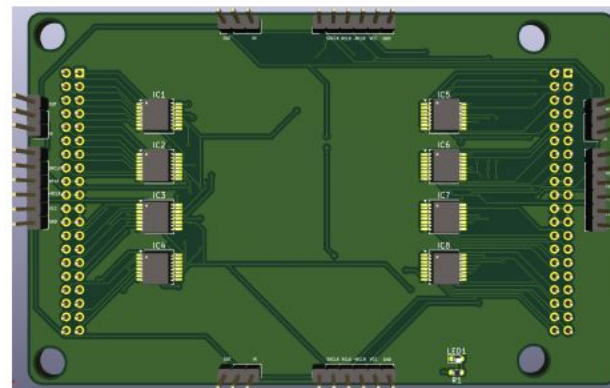
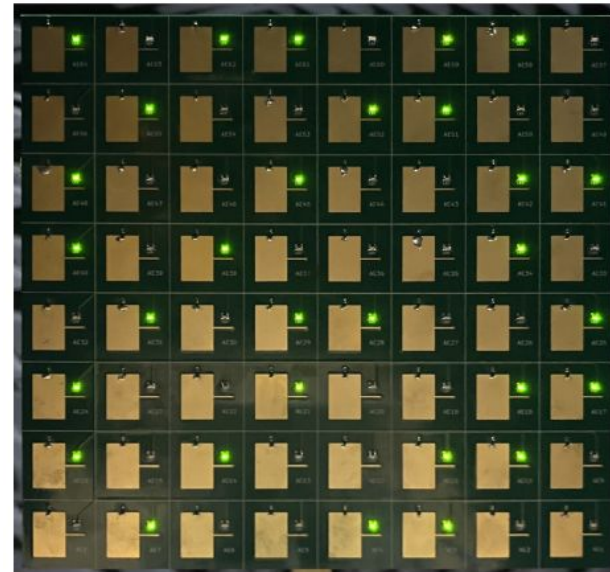
## RIS Tile

- 8x8 → 64 unit cells
  - Separated by half wavelength
- 18.45cm<sup>2</sup> area
- LEDs indicate ON state
- “Tile”? → align multiple PCBs  
→ larger RIS w/o design concerns

## Control Board

- 8 Shift Registers (1 bit per cell)
- SPI interface → ESP32
- Holds tile itself with two 40-pin connectors

Design has contributed to standardization efforts in RIS technology.





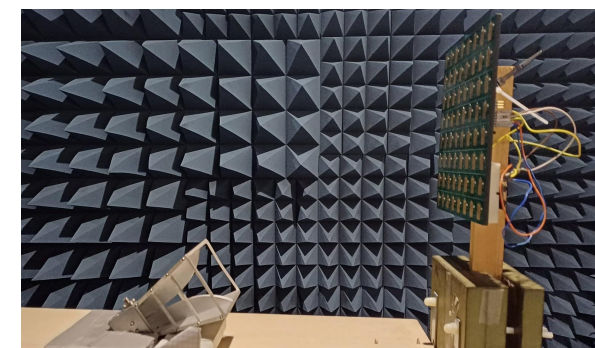
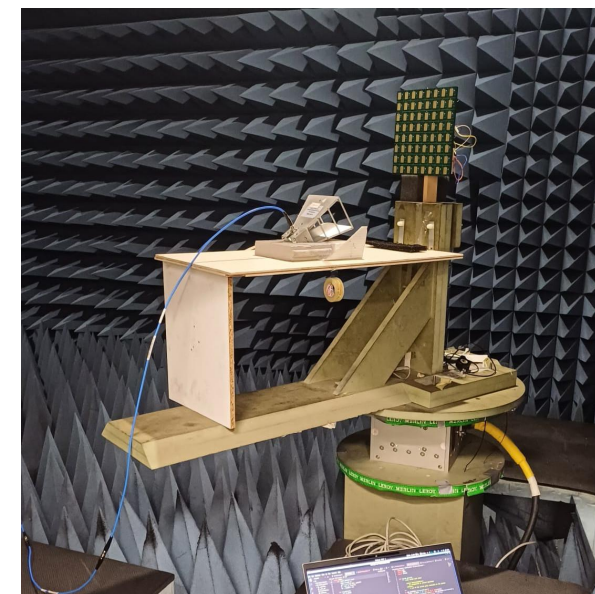
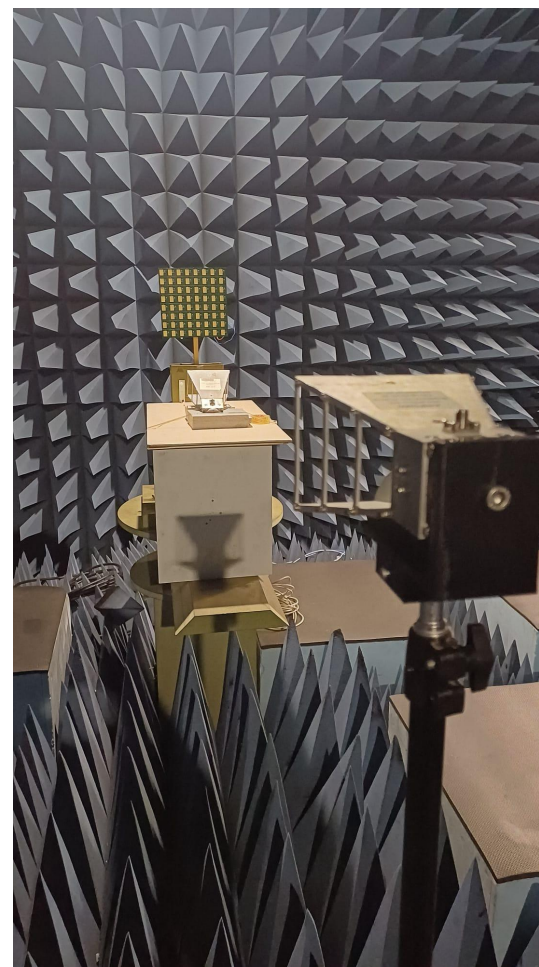
# 8×8 RIS Tile Design and Beamforming

## Objective:

- Measure S21 parameters for various RIS control patterns and orientations.
- Validate **RIS beamforming capabilities** under controlled conditions.

## Experimental Setup

- Anechoic chamber (7 m × 7 m × 3 m)
- **RIS**: on rotating platform
- **Tx**: 25.5 cm along X-axis and 36.5 cm along Z-axis (40 cm total distance)
- **Rx**: 170 cm from RIS
- Automated data acquisition:
  - RIS Steering:  $0^\circ$ ,  $\pm 20^\circ$ ,  $\pm 40^\circ$
  - Rotor Orientation:  $\pm 60^\circ$



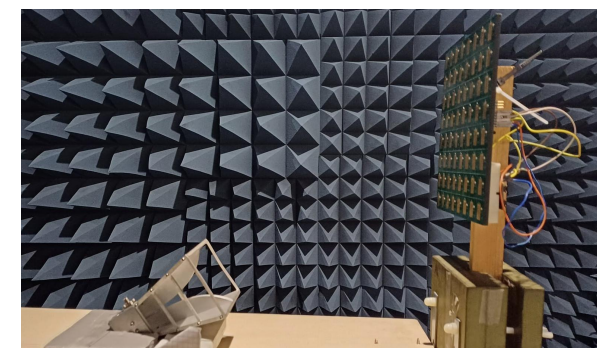
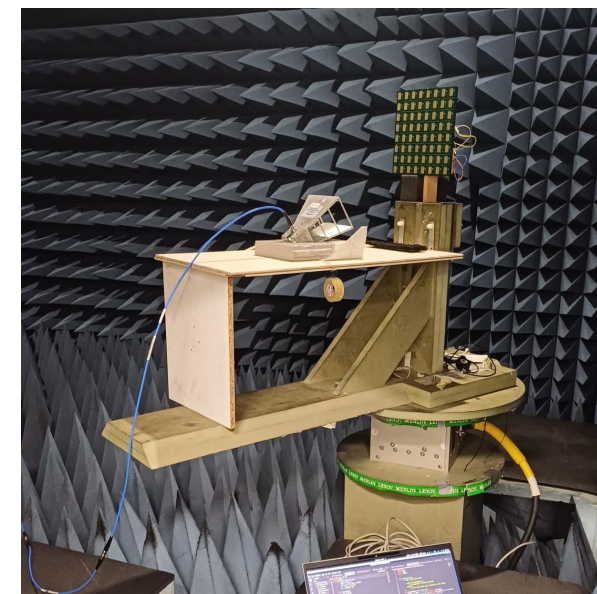
# 8×8 RIS Tile Design and Beamforming

## Objective:

- Measure S21 parameters for various RIS control patterns and orientations.
- Validate **RIS beamforming capabilities** under controlled conditions.

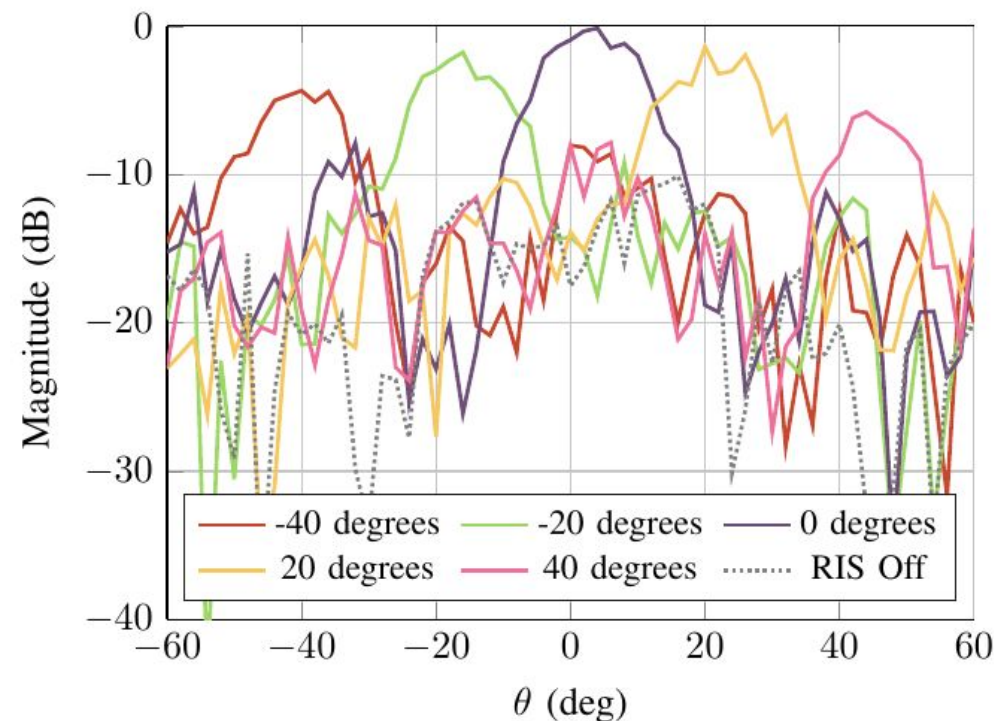
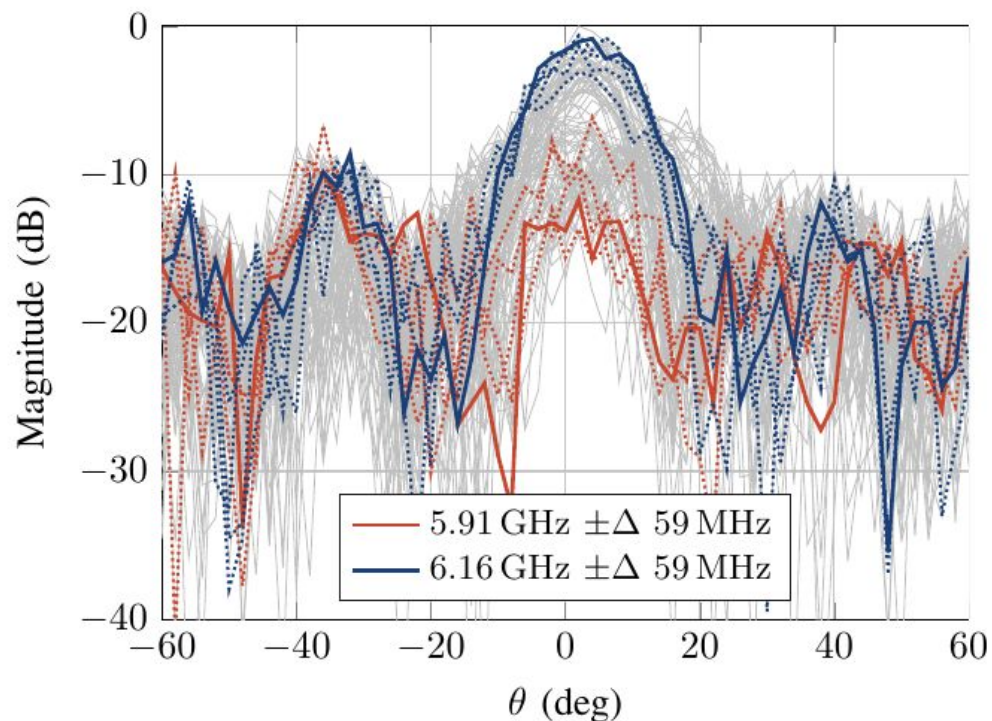
## Experimental Setup

- Anechoic chamber (7 m × 7 m × 3 m)
- **RIS**: on rotating platform
- **Tx**: 25.5 cm along X-axis and 36.5 cm along Z-axis (40 cm total distance)
- **Rx**: 170 cm from RIS
- Automated data acquisition:
  - RIS Steering:  $0^\circ, \pm 20^\circ, \pm 40^\circ$
  - Rotor Orientation:  $\pm 60^\circ$





# 8×8 RIS Tile Design and Beamforming



## Experimental Results

(left)  $\pm 50$  MHz bandwidth centered at 6.16 GHz shows the most pronounced steering response, despite chosen frequency of 5.91 GHz. Likely due to inaccuracies in physical setup.

(right) Beamsteering patterns clearly observed across the 5.0–6.5 GHz range.

## Conclusion

RIS correctly beamforms for 5.0–6.5 GHz, validating capability of controlling medium. Broadband influence of RIS supports application to hand gesture recognition (HGR).

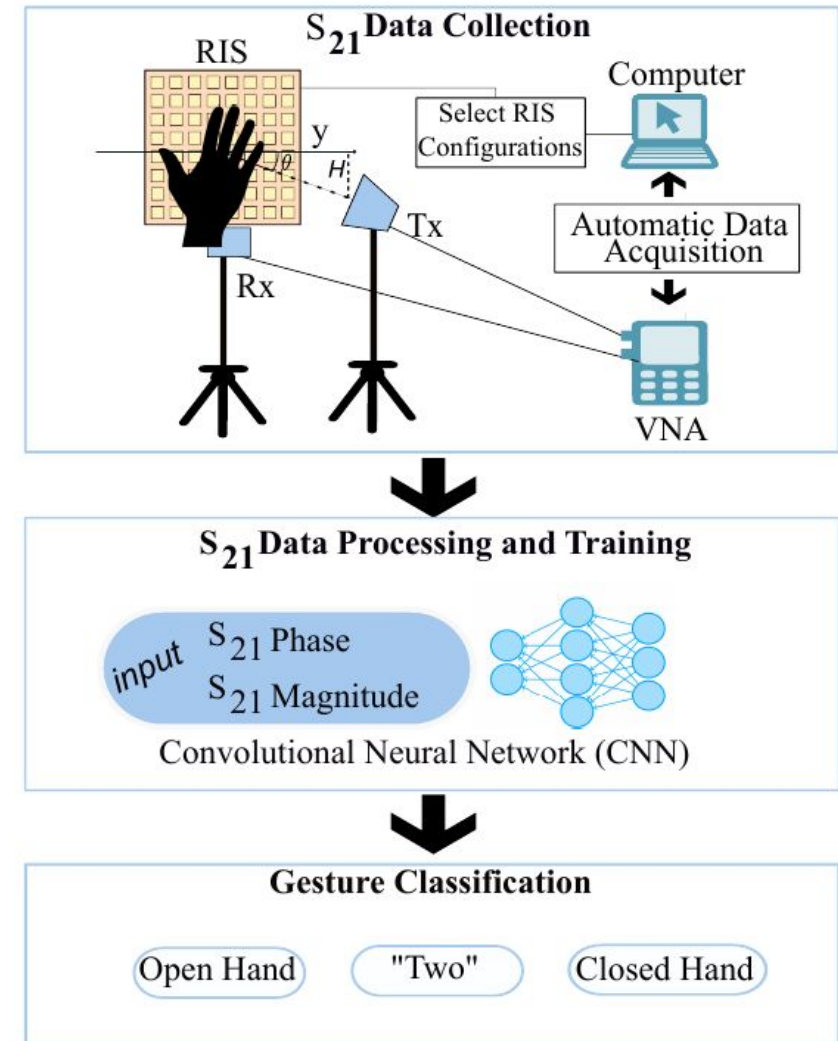
# RIS-Based Hand Gesture Recognition (HGR)

## Setup

- ~~1. Physical setup for HGR~~
- ~~2. Channel model and RIS configuration~~

## Experiments

- ~~3. Unit cell characterization~~
- ~~4. RIS steering validation~~
- 5. Feasibility study of HGR with RIS**
6. RIS-based HGR Classification



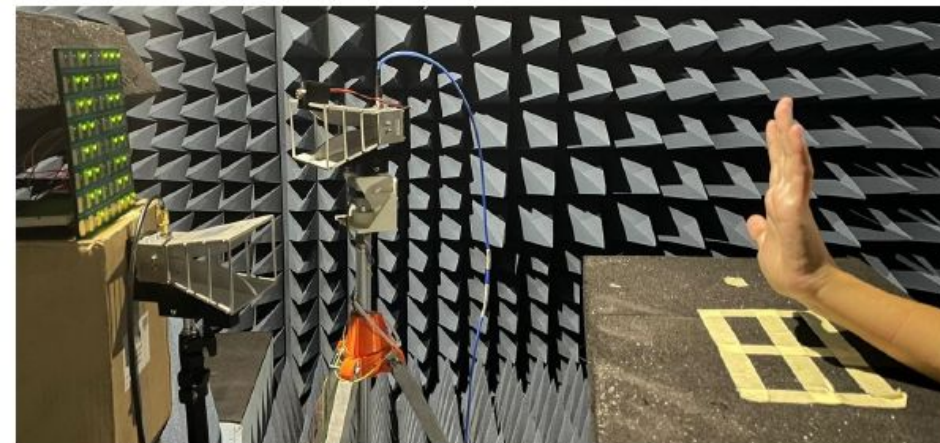
# RIS-Based HGR Feasibility

## Objective:

Validate the experimental setup and methodology for RIS-based HGR, and test if S21 parameters can distinguish different hand gestures in the Sol.

## Experimental Setup

- Anechoic chamber (7 m × 7 m × 3 m)
- Tx and Rx → two pyramidal horns
- Setup according to the model
- RIS: four steering angles (5°, 10°, 15°, 20°)
  - No configuration sequences
- Sol: three different static hand gestures
- Dataset
  - 1 subject × 3 gestures × 5 RIS configs.
  - Frequency range: 5.0 GHz to 6.5 GHz





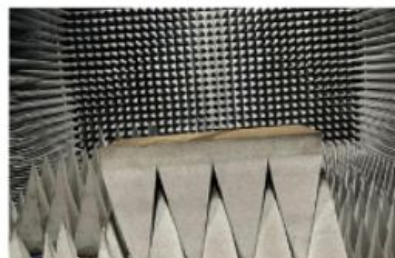
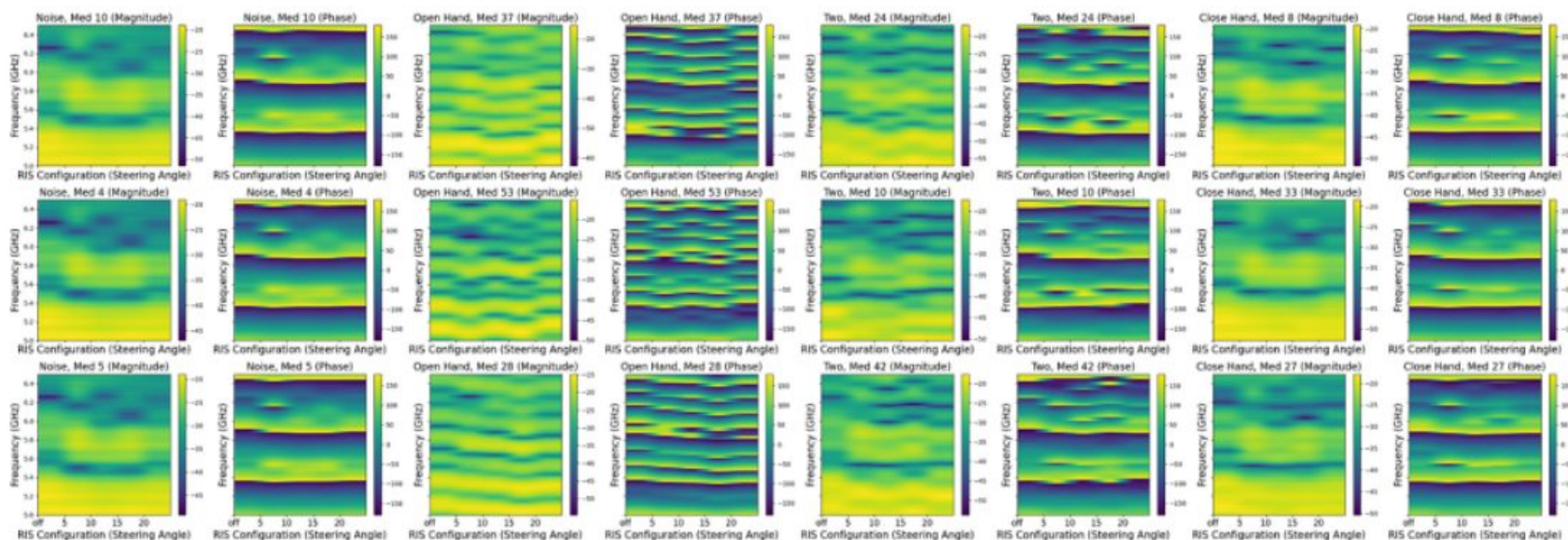
# RIS-Based HGR Feasibility

## Experimental Results

Consistent S21 response for all measurements of same gesture. Significant differences between gestures in both phase and magnitude responses.

## Conclusion

RIS-based HGR is feasible, with clear gesture differentiation in S21 data. Future experiments will use a proxy hand model to streamline data gathering.



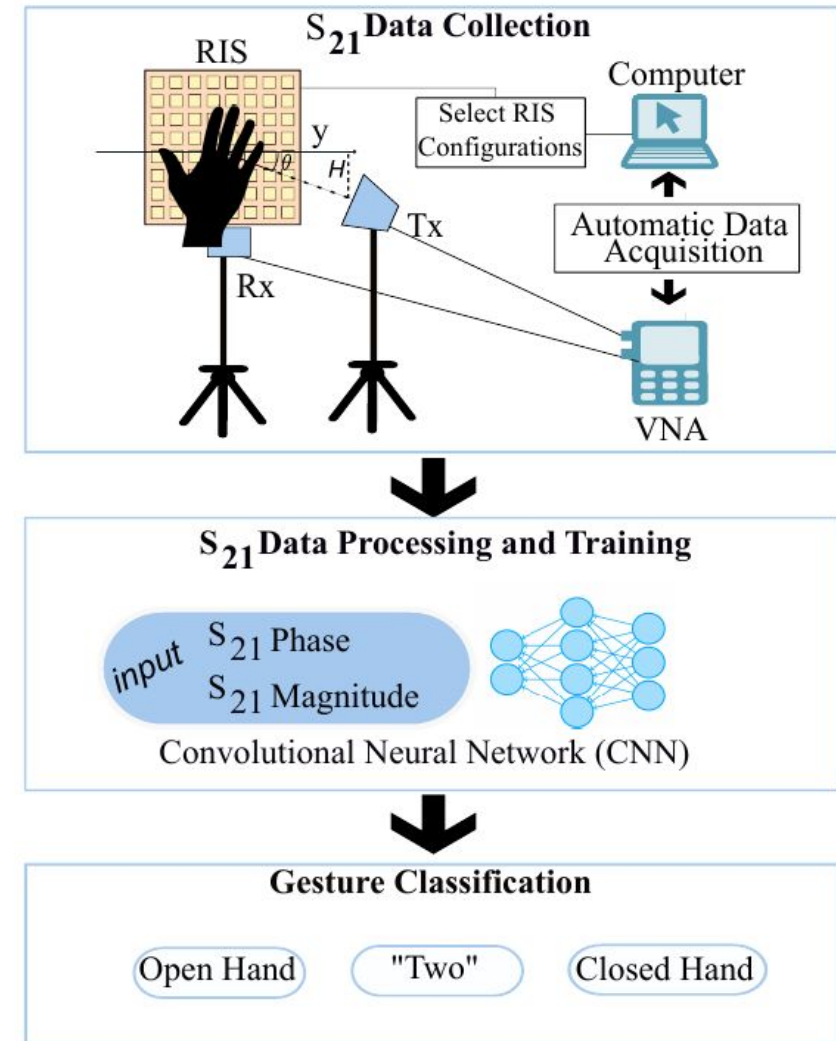
# RIS-Based Hand Gesture Recognition (HGR)

## Setup

- ~~1. Physical setup for HGR~~
- ~~2. Channel model and RIS configuration~~

## Experiments

- ~~3. Unit cell characterization~~
- ~~4. RIS steering validation~~
- ~~5. Feasibility study of HGR with RIS~~
- 6. RIS-based HGR Classification**



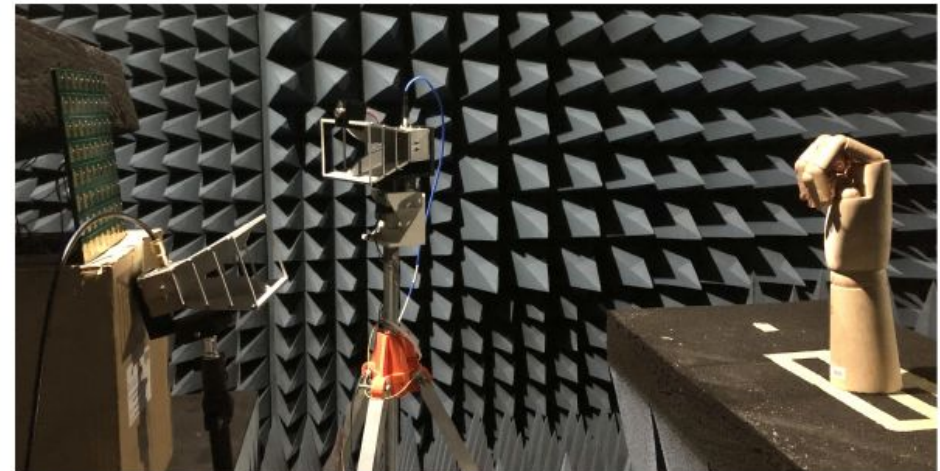
# RIS-Based HGR Classification: Data

## Objective:

Validate RIS-based hand gesture classification using a large dataset, compare random RIS config. sequences to FCAO-optimized sequences, and classify gestures with S21 data.

## Experimental Setup

- Model hand in same 3 gestures
- Applied sequence RIS
  - Random, and FCAO optimized
- Frequency range: 5 GHz to 6.5 GHz
- 115 runs  $\times$  10 RIS frames (390 configs./run).
- Total: ~3105 samples per gesture (random and optimized configurations).
- Total data acquisition time: **~39 hours**.





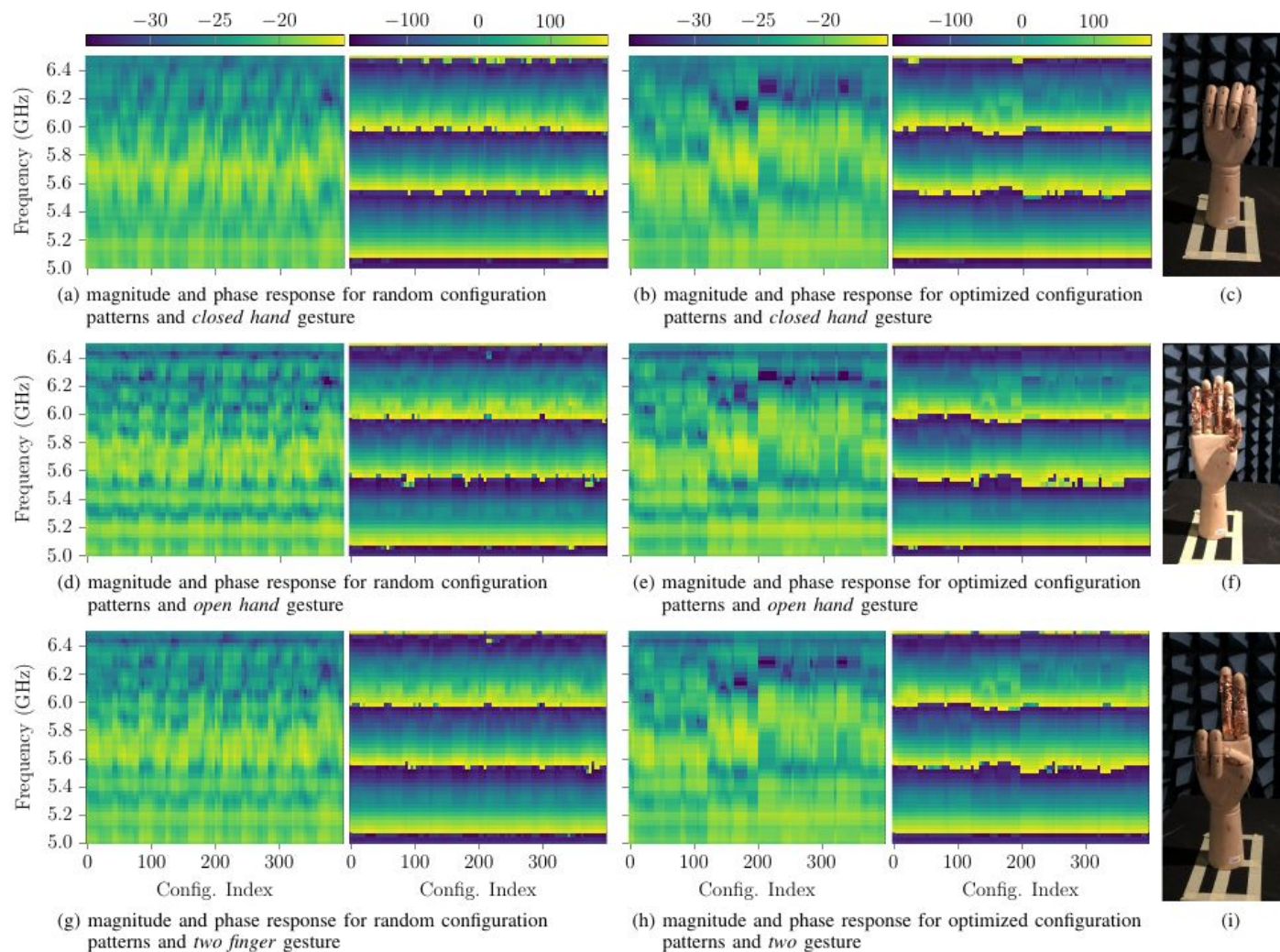
# RIS-Based HGR Classification: Data

## Optimized vs. Random Configurations:

- Random: Small variability in magnitude across during sequence. Slight phase variability.
- Optimized: captured more distinct S21 responses across gestures.
- Faster CNN learning and improved classification accuracy with optimized data.
- All measurements for same gesture very similar.

## Data Augmentation for learning

Hand repositioned in 8 minor orientations for each gesture, and noise was synthetically added to the samples.



random

optimized

# RIS-Based HGR Classification: CNN

## Model 1 (Narrowband):

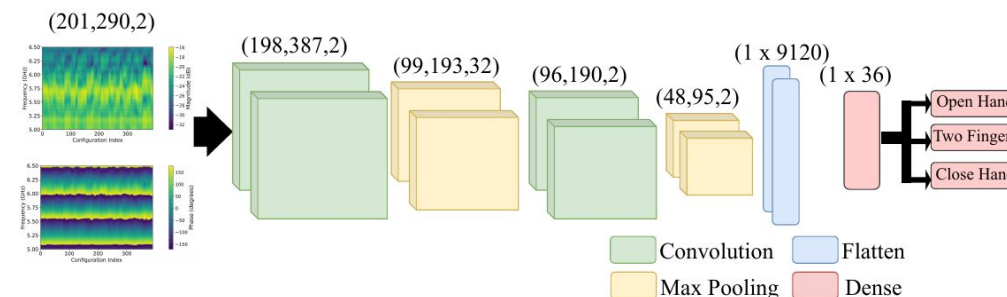
Input: Average S21 response per frame at 5.91 GHz. Optimized configuration sequences improved accuracy by 3.53%.

## Model 2 (Broadband):

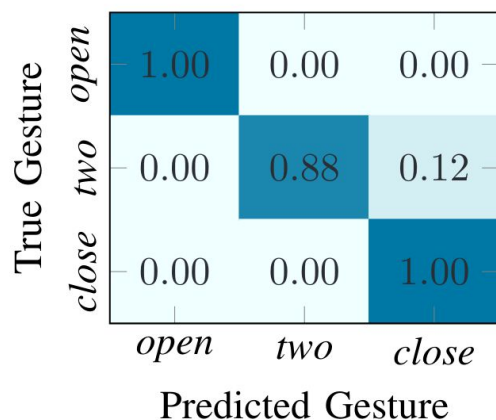
Input: Magnitude and phase over 5–6.5 GHz. High accuracy for both configuration sequences (~99%), with minimal gains for optimization.

## Conclusion

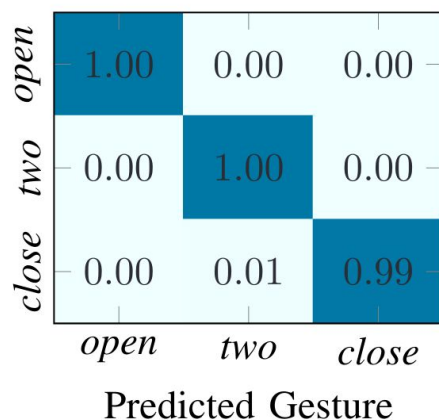
Successful HGR classification with both models. Narrowband model benefits from from optimized configuration sequences. Broadband model can capture mode information, and benefits less from optimized sequences.



CNN Model #2

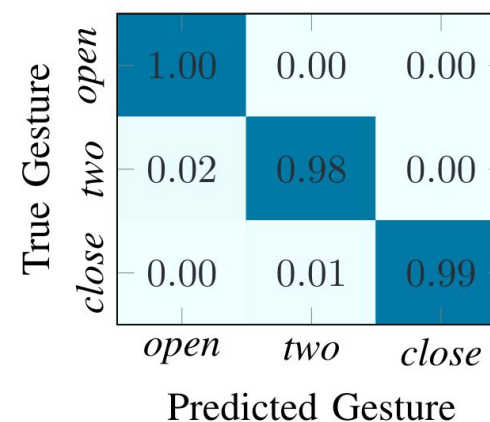


(a) CNN #1 and random config.

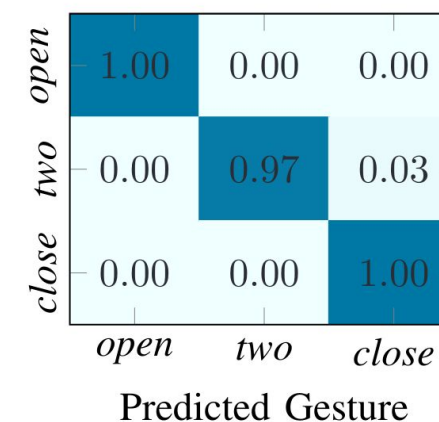


(b) CNN #1 and optimized config.

CNN Model #1 Results



(a) CNN #2 and random config.



(b) CNN #2 and optimized config.

CNN Model #2 Results

# Conclusions

- **Advancing RF-based Hand Gesture Recognition with RIS**
  - Demonstrated RF-based classification of three distinct gestures using RIS technology
  - Designed and validated an 8×8 RIS tile for the WiFi-6E range, with successful beam steering at 6.16 GHz
  - Published dataset for RF-based HAR
- **Future:**
  - Assemble larger RIS with 4 tiles, and aim for higher frequencies
  - Expand Space-of-Interest for Human Posture Recognition



Campus da Faculdade de  
Engenharia da  
Universidade do Porto

Rua Dr. Roberto Frias

4200-465 Porto, Portugal

T +351 222 094 000

[info@inesctec.pt](mailto:info@inesctec.pt)

[www.inesctec.pt](http://www.inesctec.pt)

